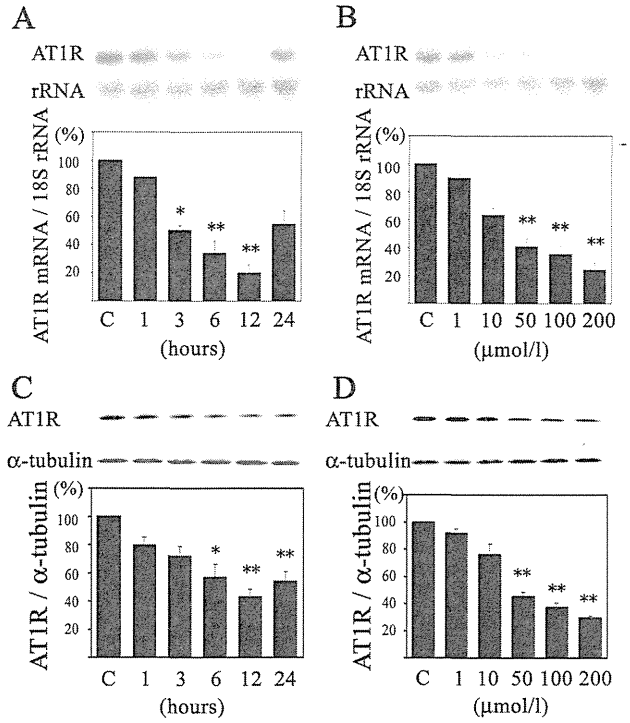

Figure 1. Suppression of AT1R mRNA and protein expression by resveratrol in VSMCs. A and C, VSMCs were incubated with resveratrol for varying periods indicated in the figure (n=6 to 7). B and D, VSMCs were incubated with resveratrol at varying concentrations for 12 hours (n=6 to 8). A and B, Expression of AT1R mRNA was determined by Northern blot analysis. C and D, Expression of AT1R protein was detected by Western blot analysis. Values are expressed as a percent of control (C) culture (100%). *P<0.05, **P<0.01 vs Control.

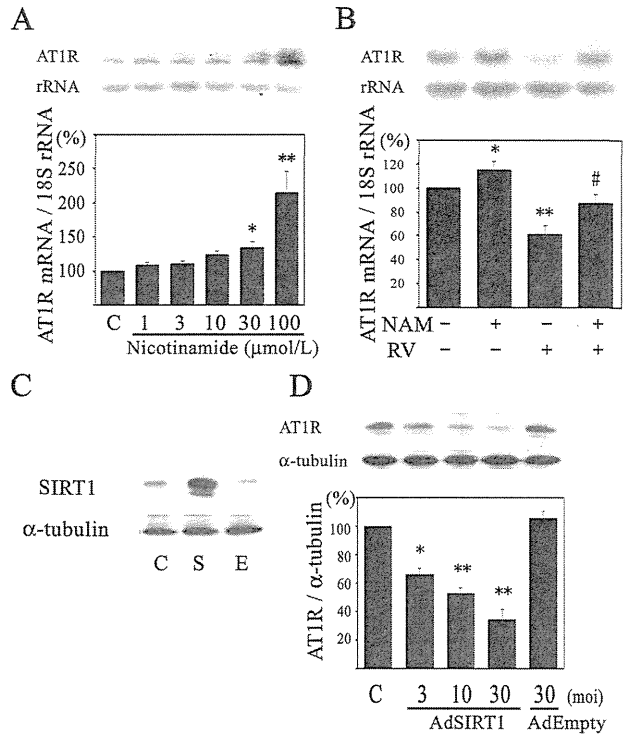

Figure 2. SIRT1 mediates downregulation of AT1R mRNA expression. A, VSMCs were incubated with nicotinamide at varying concentrations for 6 hours (n=6). B, VSMCs were incubated with resveratrol and/or nicotinamide for 12 hours (n=8). Expression level of AT1R mRNA was examined. C, VSMCs were infected with AdSIRT1 or AdEmpty and expression of SIRT1 was examined. D, VSMCs infected with AdSIRT1 or AdEmpty. Expression of AT1 protein was examined. Values are expressed as a percent of control (C) culture (100%). *P<0.05, **P<0.01, vs C. #P<0.05 vs RV.

Results

Resveratrol Suppresses AT1R Expression in VSMCs

VSMCs were incubated with resveratrol (100μmol/L) for varying time periods, and expression level of AT1R mRNA was determined by Northern blot analysis. The expression level of AT1R mRNA was significantly reduced by resveratrol at 6 hours compared with the control level, and the reduction was reached a maximum at 12 hours of stimulation (Figure 1A). Incubation with varying concentrations of resveratrol resulted in downregulation of AT1R mRNA in a dose-dependent manner (Figure 1B). Western blot analysis revealed that resveratrol (100μmol/L) reduced AT1R protein level in VSMCs. The reduction was reached a maximum at 12 to 24 hours (Figure 1C), and resveratrol downregulated AT1R protein in a dose-dependent manner (Figure 1D). To exclude a possible toxic effect of resveratrol on VSMC, we next assessed cell viability by trypan blue staining. VSMCs were incubated with resveratrol (200μmol/L) for 24 hours. Resveratrol did not decrease the viability of VSMCs (in percent of viable cells: Control 97.7±2.0%, Resveratrol 98.3±1.0%, not significant n=4). In addition, resveratrol did not affect SIRT1 expression level (supplemental Figure I, available online at http://atvb.ahajournals.org).

SIRT1 Mediates AT1R mRNA Downregulation

Resveratrol is known to activate SIRT1. We examined whether SIRT1 is involved in the resveratrol-induced AT1R downregulation. The expression level of AT1R mRNA was significantly increased by incubation with nicotinamide, a noncompetitive inhibitor of SIRT1 compared with the control level in a dose-dependent manner (1 to 100 μmol/L, Figure 2A). Resveratrol (RV: 50 μmol/L)-induced suppression of AT1R was significantly reversed by addition of nicotinamide (NAM, 30 μmol/L; Figure 2B). However, resveratrol downregulated AT1R mRNA in the presence of TSA, class I or II HDAC inhibitor (supplemental Figure II). To achieve high expression levels of SIRT1 in VSMCs, we used a recombinant adenovirus vector expressing wild-type of SIRT1 (S, 10 moi) and AdEmpty (E,10 moi; Figure 2C). Overexpression of SIRT1 (3 to 30 moi) significantly suppressed AT1R expression compared with the cells infected with AdEmpty (30 moi; Figure 2D). To clarify whether AT1R downregulation is functional, we examined ERK phosphorylation. AngII (100 nmol/L)-induced ERK phosphorylation was inhibited in SIRT1 overexpressing cells, but not in empty vector-infected cells, suggesting that downregulation of AT1R attenuated the response of VSMCs to AngII (supplemental Figure IIIA). However, PMA-induced ERK phosphorylation was not affected in the same condition, suggesting that the pathway to ERK activation is almost intact in SIRT1 overexpressing cells (supplemental Figure IIIB).

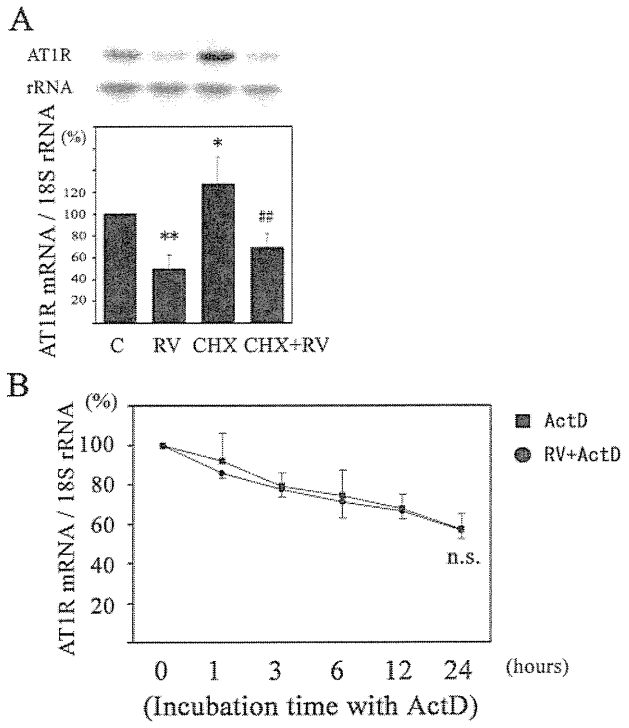

Figure 3. Effect of cycloheximide and actinomycin D on resveratrol-induced AT1R downregulation. A, Effect of cycloheximide (CHX) on resveratrol (RV)-induced AT1R mRNA downregulation was examined by Northern blot analysis. Values are expressed as a percent of control (C) culture (100%; n=8). *$P<0.05$, **$P<0.01$ vs control, ##$P<0.01$ vs CHX. B, Effect of actinomycin D (ActD) on resveratrol-induced AT1R mRNA downregulation was examined by Northern blot analysis. The expression level of AT1R mRNA in VSMCs before addition of actinomycin D in each group was set as 100% (n=5). n.s: not significant.

De Novo Protein Synthesis Is Not Required for Resveratrol-Induced Downregulation of AT1R Expression

To examine whether resveratrol-induced downregulation of AT1R mRNA requires de novo protein synthesis, we examined the effect of cycloheximide (10μmol/L). Although incubation with cycloheximide alone for 12 hours upregulated the AT1R mRNA expression, resveratrol significantly suppressed the AT1R mRNA level in the presence of cycloheximide (Figure 3A). These data suggest that resveratrol-induced AT1R downregulation does not require de novo protein synthesis. We next examined whether resveratrol affects AT1R mRNA stability. In control, AT1R mRNA levels were reduced by 50% after 24 hours, and resveratrol did not affect the degradation rate of AT1R mRNA (Figure 3B).

Resveratrol Inhibits AT1R Expression at the Transcriptional Level

To locate the DNA element responsible for resveratrol-induced AT1R suppression, we examined the transcription activity of the deletion mutants of AT1a gene promoter/luciferase fusion DNA (Figure 4A). The suppression was observed in all mutants, suggesting that the response element exists in the DNA segment between −61 bp and +25 bp, which contains Sp1 site. The luciferase construct with mutation in Sp1 site failed to respond to resveratrol, indicating the important role of Sp1 site in resveratrol-induced downregulation.

Reduction of Sp1 Binding by Resveratrol

We examined the DNA binding protein bound to the Sp1 site using gel mobility shift assay (Figure 5). When nuclear extracts from resveratrol-stimulated VSMC were used, DNA binding protein (arrow) was decreased compared with those from unstimulated VSMC (lanes 1 to 2). Addition of 50 times molar excess of unlabeled probe (lane 4) but not the Sp1 mutant probe (lane 3) eliminated this band, confirming the specificity of the binding.

Resveratrol Suppresses AT1R Expression In Vivo

Finally, we examined whether resveratrol affects AT1R expression in vivo. Nine-week-old mice were allotted to resveratrol group or water group in a random manner. Blood pressure, heart rate, and body weight were not significantly different between resveratrol- and water-treated mice after 1 week (supplemental Table I). After 1 week, membrane protein of aorta was extracted and Western blot analysis was performed. Western blot revealed that resveratrol reduced expression level of AT1R protein in the aorta (Figure 6A). And

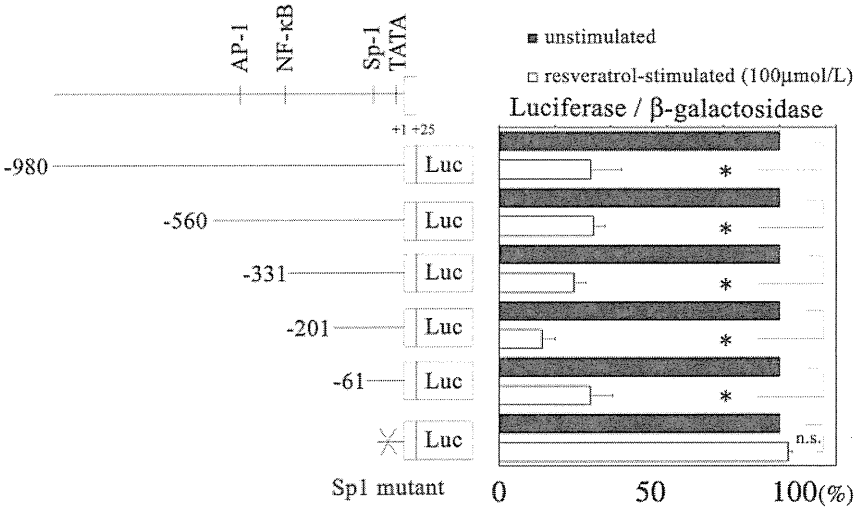

Figure 4. Resveratrol downregulates AT1R mRNA expression through transcriptional mechanisms. Left, The scheme of deletion mutants of AT1R promoter/luciferase fusion DNA construct and Sp1 mutant construct is shown. Right, The bar graphs indicate luciferase activity normalized by β-galactosidase activity derived from the corresponding deletion or Sp1 mutant. The luciferase activity of resveratrol-stimulated VSMCs (white bars) relative to unstimulated VSMCs (black bars) in each group is indicated. Values (mean±SEM) are expressed as a percent (n=6). *$P<0.01$ vs unstimulated.

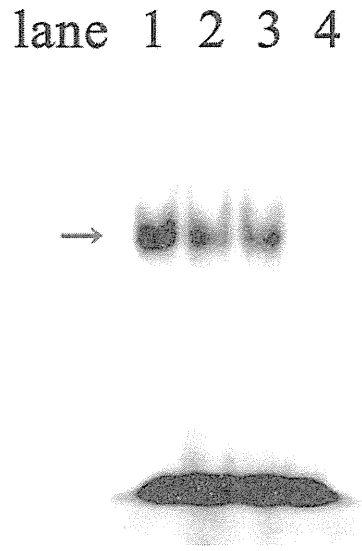

Figure 5. Gel mobility shift assay of nuclear protein of VSMCs. Binding activity of AT1R gene promoter (−40 bp to −6 bp), containing Sp1 site, was examined in the nuclear protein from unstimulated (lane 1) or resveratrol (100 μmol/L)-stimulated (lane2) VSMCs, by gel mobility shift assay. Fifty times molar excess of unlabeled mutant probe or wild-type probe were added to the reaction mixture (lane 3 and 4, respectively).

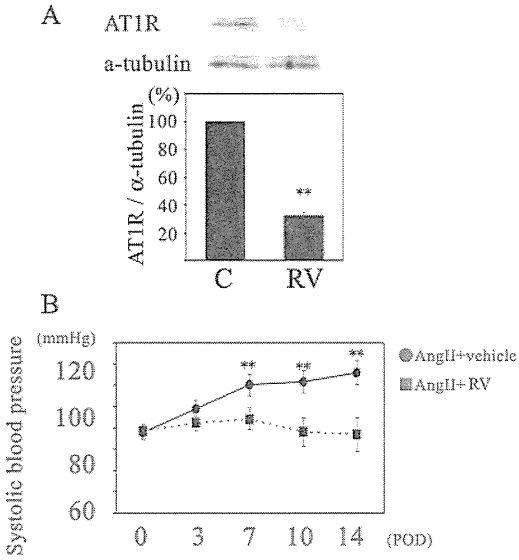

Figure 6. Effect of resveratrol on AT1R protein expression in the mouse aorta. A, AT1R expression in the membrane fractions of the aorta of mice treated with either resveratrol (RV) or water (C) was analyzed with Western blot analysis. The values are expressed as a percentage of water treated group (100%; n=4). $^{**}P<0.01$ vs water-treated group. B, Mice were treated with either resveratrol or vehicle (water). Ang II was administered in both groups and blood pressure was measured (n=4). $^{**}P<0.01$ vs vehicle-treated group. POD indicates postoperative days after implantation of osmotic minipump.

then, we examined the effect of resveratrol on AngII-induced hypertension. We found that Ang II–induced hypertension was markedly blunted by resveratrol administration (Figure 6B). Heart rate and body weight were not significantly different between Ang II+vehicle and Ang II+resveratrol-treated mice after 2 weeks (supplemental Table II).

Discussion

In the present study, we demonstrated that resveratrol reduced the expression of AT1R in VSMCs and in mice aorta. Resveratrol reduced AT1R promoter activity without an effect on mRNA stability. Overexpression of SIRT1 suppressed AT1R expression, and nicotinamide increased AT1R expression. To our knowledge, this is the first report showing the downregulation of vascular AT1R by resveratrol. Furthermore, we demonstrated that SIRT1 overexpression suppressed Ang II–induced ERK phosphorylation, suggesting that downregulation of AT1R attenuated AT1R signaling.

We showed that nicotinamide, a SIRT1 natural inhibitor, upregulated the expression level of AT1R mRNA, and overexpression of SIRT1 significantly suppressed AT1R protein expression. Furthermore, resveratrol-induced suppression of AT1R was reversed by nicotinamide. These data suggested that resveratrol suppressed AT1R expression through SIRT1 activation at least in part.

Haider UG et al reported that resveratrol interfered with Ang II signaling pathways in VSMCs.[29] Resveratrol inhibited Ang II–induced tyrosine-phosphorylation of Gab1 and its association with the p85 subunit of phosphatidylinositol-3-kinase. Therefore, resveratrol inhibits AT1R signaling as well as gene expression. Actis-Goretta L reported that red wine inhibits ACE activity more effectively than white wine. However resveratrol was ineffective in the inhibition of ACE activity in rat tissues.[30] We supposed that resveratrol may suppress renin-angiotensin system not via ACE downregulation but via AT1R downregulation and inhibition of AT1R signaling.

In a rat model of injured aorta, administration of resveratrol accelerated reendothelialization and inhibited neointimal formation.[31] Because Ang II and AT1R play an important role in the neointimal formation after vascular injury, downregulation of AT1R expression by resveratrol may be involved in the suppression of neointimal formation. In addition, resveratrol has been reported to inhibit serum-induced VSMC growth.[32] Therefore, direct inhibition of VSMC growth by resveratrol may also play a role.

It was previously reported that resveratrol increased the endothelial nitric oxide synthase (eNOS) mRNA stability in human EA.hy 926 endothelial cells.[33] We investigated whether resveratrol affects the AT1R mRNA stability in VSMCs. Resveratrol reduced AT1R gene promoter activity, but resveratrol did not affect AT1R mRNA stability. These data suggest that resveratrol suppressed AT1R gene expression at the transcriptional level rather than posttranscriptional level. The deletion analysis of the AT1R gene promoter revealed that suppression of AT1R expression by resveratrol is dependent on the most proximal promoter region (from −61 bp to +25 bp), which contains Sp1 binding site (GC box). The luciferase construct with mutation in GC box failed to respond to resveratrol, indicating an important role of Sp1 site in resveratrol-induced AT1R downregulation. Gel shift assay showed that DNA binding protein bound to the Sp1 site was decreased in resveratrol-stimulated VSMC. A recent report showed that Sp1 is constitutively acetylated at Lys703,[34] and deacetylation of Sp1 induced activation of

12(s)-lipoxygenase gene expression. Conversely, another report showed that HDAC1 mediates repression of transforming growth factor (TGF) β type II receptor gene transcription by deacetylation of Sp1.[35] Therefore, the effects of deacetylation of Sp1 on gene expression may be context-dependent. Our data suggest that resveratrol inhibits Sp1 binding to AT1R gene promoter and AT1R gene transcription, supporting the results of the latter report. However, it is not clear how SIRT1 inhibits Sp1 binding at this moment, and further study is needed.

As shown in Figure 6B, chronic low-dose AngII infusion via osmotic minipump developed hypertension in mice as described previously,[36] and Ang II–induced hypertension was blunted by resveratrol. Because resveratrol inhibits AT1R signaling,[29] we supposed that this was attributable to inhibition of AT1R signaling and AT1R downregulation as shown Figure 6A by resveratrol. However, it is difficult to dissect these 2 effects in terms of the blood pressure regulation.

Previous studies have demonstrated that resveratrol extends the life span of diverse species.[6,7] It was also reported that inhibition of Ang II function by angiotensin converting enzyme inhibitor[37] and AT1R antagonist[22] prolonged the lifespan of hypertensive rats. Considering that oral administration of resveratrol suppressed the AT1R protein expression in the aorta of mice, the inhibition of the renin-angiotensin system via AT1R suppression may contribute, at least in part, to the longevity by resveratrol. The downregulation of AT1R may also account for antiatherogenic effect of resveratrol.

In conclusion, we demonstrated that resveratrol downregulated AT1R expression through SIRT1. The suppression of AT1R expression may contribute to resveratrol-induced lifespan extension, inhibition of atherosclerosis and inflammation.

Sources of Funding

This study was supported in part by Grants-in-aid for Scientific Research from the Ministry of Education, Culture, Sports, Science, and Technology of Japan (19590867) and Kimura Foundation Research Grant 2007 to T.I.

Disclosures

None.

References

1. Soleas GJ, Diamandis EP, Goldberg DM. Wine as a biological fluid: history, production, and role in disease prevention. *J Clin Lab Anal.* 1997; 11:287–313.
2. Nonomura S, Kanagawa H, Hashimoto A. Chemical constituents of polygonaceous plants. Studies on the components of Ko-jo-kon(*Polygonum Caspidatum* Sieb. *et Zucc) Yakugaku Zasshi.* 1963;83: 988–990.
3. Baur JA, Sinclair DA. Therapeutic potential of resveratrol: the in vivo evidence. *Nat Rev Drug Discov.* 2006;5:493–506.
4. Wang Q, Xu J, Rottinghaus GE, Lubahn D, Sun GY, Sun AY. Resveratrol protects against global cerebral ischemic injury in gerbils. *Brain Res.* 2002;958:439–447.
5. Jang M, Cai L, Udeani GO, Slowing KV, Thomas CF, Beecher CW, Fong HH, Farnsworth NR, Kinghorn AD, Mehta RG, Moon RC, Pezzuto JM. Cancer chemopreventive activity of resveratrol, a natural product derived from grapes. *Science.* 1997;275:218–220.
6. Howitz KT, Bitterman KJ, Cohen HY, Lamming DW, Lavu S, Wood JG, Zipkin RE, Chung P, Kisielewski A, Zhang LL, Sscherer B, Sinclair DA. Small molecule activators of sirtuins extend Saccharomyces cerevisiae lifespan. *Nature.* 2003;425:191–196.
7. Valenzano DR, Terzibasi E, Genade T, Cattaneo A, Domenici L, Cellerino A. Resveratrol prolongs lifespan and retards the onset of age-related markers in a short-lived vertebrate. *Curr Biol.* 2006;16: 296–300.
8. Baur JA, Pearson KJ, Price NL, Jamieson HA, Lerin C, Kalra A, Prabhu VV, Allard JS, Lopez-Lluch G, Lewis K, Pistell PJ, Poosala S, Becker KG, Boss O, Gwinn D, Wang M, Ramaswamy S, Fishbein KW, Spencer RG, Lakatta EG, Le Couteur D, Shaw RJ, Navas P, Puigserver P, Ingram DK, de Cabo R, Sinclair DA. Resveratrol improves health and survival of mice on a high-calorie diet. *Nature.* 2006;444:337–342.
9. Okamoto H, Fujioka Y, Takahashi A, Takahashi T, Taniguchi T, Ishikawa Y, Yokoyama M. Trichostatin A, an inhibitor of histone deacetylase, inhibits smooth muscle cell proliferation via induction of p21(WAF1). *J Atheroscler Thromb.* 2006;13:183–191.
10. Denu JM. Linking chromatin function with metabolic networks: Sir2 family of NAD(+)-dependent deacetylases. *Trends Biochem Sci.* 2003; 28:41–48.
11. Imai S, Christopher MA, Matt K, Leonard G. Transcriptional silencing and longevity protein Sir2 is an NAD-dependent histone deacetylase. *Nature.* 1999;403:795–800.
12. Bitterman KJ, Anderson RM, Cohen HY, Latorre-Esteves M, Sinclair DA. Inhibition of silencing and accelerated aging by nicotinamide, a putative negative regulator of yeast sir2 and human SIRT1. *J Biol Chem.* 2002;277:45099–45107.
13. Dryden SC, Nahhas FA, Nowak JE, Goustin AS, Tainsky MA. Role for human SIRT2 NAD-dependent deacetylase activity in control of mitotic exit in the cell cycle. *Mol Cell Biol.* 2003;23:3173–3185.
14. Blander G, Guarente L. The Sir2 family of protein deacetylases. *Annu Rev Biochem.* 2004;73:417–435.
15. Cohen HY, Miller C, Bitterman KJ, Wall NR, Hekking B, Kessler B, Howitz KT, Gorospe M, de Cabo R, Sinclair DA. Calorie restriction promotes mammalian cell survival by inducing the SIRT1 deacetylase. *Science.* 2004;305:390–392.
16. Goodfriend TL, Elliott ME, Catt KJ. Drug therapy: angiotensin receptors and their antagonists. *N Engl J Med.* 1996;334:1649–1654.
17. Sasaki K, Yamano Y, Bardhan S, et al. Cloning and expression of a complementary DNA encoding a bovine adrenal angiotensin II type-1 receptor. *Nature.* 1991;351:230–233.
18. Kambayashi Y, Bardhan S, Takahashi K, et al. Molecular cloning of a novel angiotenin II receptor isoform involved in phosphotyrosine phosphatase inhibition. *J Biol Chem.* 1993;268:24543–24546.
19. Horiuchi M, Akishita M, Dzau VJ. Recent progress in angiotensin II type 2 receptor research in the cardiovascular system. *Hypertension.* 1999;33: 613–621.
20. Touyz RM, Schiffrin EL. Signal transduction mechanisms mediating the physiological and pathophysiological actions of angiotensin II in vascular smooth muscle cells. *Pharmacol Rev.* 2000;52:639–672.
21. Paradis P, Dali-Youcef N, Paradis FW, Thibault G, Nemer M. Overexpression of angiotensin II type 1 receptor in cardiomyocytes induces cardiac hypertrophy and remodeling. *Proc Natl Acad Sci U S A.* 2000; 97:931–936.
22. Wolfgang L, Holger H, Bernward AS, Gabriele W. Long-term angiotensin II type 1 receptor blockade with Fonsartan doubles lifespan of hypertensive rats. *Hypertension.* 2000;35:908–913.
23. Ichiki T, Usui M, Kato M, Funakoshi Y, Ito K, Egashira K, Takeshita A. Downregulation of angiotensin II type 1 receptor gene transcription by nitric oxide. *Hypertension.* 1998;31:342–348.
24. Imayama I, Ichiki T, Inanaga K, Ohtsubo H, Fukuyama K, Ono H, Hashiguchi Y, Sunagawa K. Telmisartan downregulates angiotensin II type 1 receptor through activation of peroxisome proliferator-activated receptorγ. *Cardiovasc Res.* 2006;72:184–190.
25. Guo DF, Uno S, Ishihata A, Nakamura N, Inagami T. Identification of a *cis*-acting glucocorticoid responsive element in the rat angiotensin II type 1A promoter. *Circ Res.* 1995;77:249–257.
26. Tokunou T, Ichiki T, Takeda K, Funakoshi Y, Iino N, Shimokawa H, Egashira K, Takeshita A Thrombin induces interleukin-6 expression through the cAMP response element in vascular smooth muscle cells. *Arterioscler Thromb Vasc Biol.* 2001;21:1759–1763.
27. Fukuyama K, Ichiki T, Takeda K, Tokunou T, Iino N, Masuda S, Ishibashi M, Egashira K, Shimokawa H, Hirano K, Kanaide H, Takeshita A. Downregulation of vascular angiotensin II type 1 receptor by thyroid hormone. *Hypertension.* 2003;41:598–603.

28. Alcendor RR, Kirshenbaum LA, Imai S, Vatner SF, Sadoshima J. Silent information regulator 2alpha, a longevity factor and class III histone deacetylase, is an essential endogenous apoptosis inhibitor in cardiac myocytes. *Circ Res*. 2004;95:971–980.
29. Haider UG, Roos TU, Kontaridis MI, Neel BG, Sorescu D, Griendling KK, Vollmar AM, Dirsch VM, Resveratrol inhibits angiotensin II- and epidermal growth factor-mediated Akt activation: role of Gab1 and Shp2. *Mol Pharmacol*. 2005;68:41–48.
30. Actis-Goretta L, Ottaviani JI, Fraga CG. Inhibition of angiotensin converting enzyme activity by flavanol-rich foods. *J Agric Food Chem*. 2006;54:229–234.
31. J G, Cq W, Hh F, Hy D, Xl X, Ym X, By W, Dj H. Effects of resveratrol on endothelial cells and their contributions to reendothelialization in intima-injured rats. *J Cardiovasc Pharmacol*. 2006;47:711–721.
32. Mnjoyan ZH, Fujise K. Profound negative regulatory effects by resveratrol on vascular smooth muscle cells: a role of p53-p21(WAF1/CIP1) pathway. *Biochem Biophys Res Commun*. 2003;311:546–552.
33. Das S, Fraga CG, Das DK. Cardioprotective effect of resveratrol via HO-1 expression involves p38 map kinase and PI-3-kinase signaling, but does not involve NFkappaB. *Free Radic Res*. 2006;40:1066–1075.
34. Hung JJ, Wang YT, Chang WC. Sp1 deacetylation induced by phorbol ester recruits p300 to activate 12(S)-lipoxygenase gene transcription. *Mol Cell Biol*. 2006;26:1770–1785.
35. Zhao S, Venkatasubbarao K, Li S, Freeman JW. Requirement of a specific Sp1 site for histone deacetylase-mediated repression of transforming growth factor β type II receptor expression in human pancreatic cancer cells. *Cancer Research*. 2003;63:2624–2630.
36. Tomasz JG, Nyssa EH, Kathryn AB, Louise AM, Ayaz R, Sergey D, Jorg G, Cornelia W, and David GH. Role of the T cell in the genesis of angiotensin II–induced hypertension and vascular dysfunction. *J Exp Med*. 2007;204:2449–2460.
37. Linz W, Jessen T, Becker RHA, Schölkens BA, Wiemer G. Long-term ACE inhibition doubles lifespan of hypertensive rats. *Circulation*. 1997; 96:3164–3172.

Supplementary Figure 1

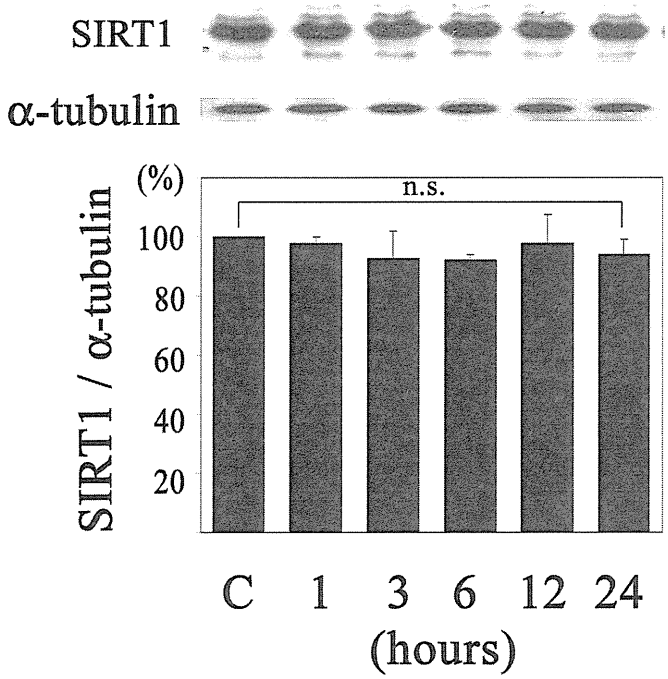

Supplementary Figure 2

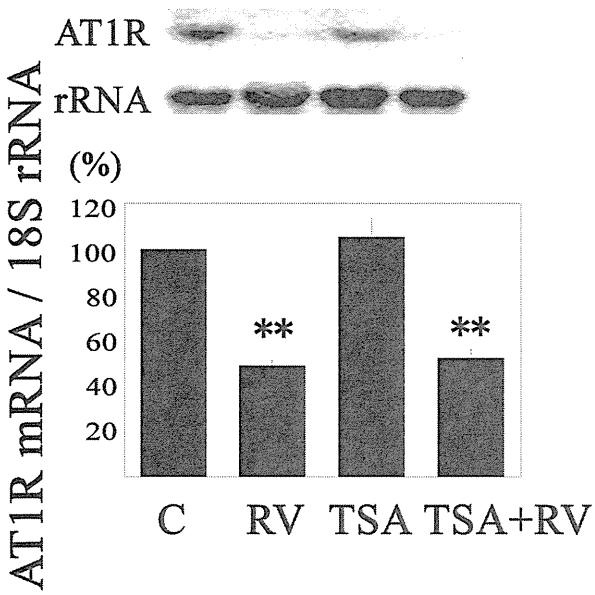

Supplementary figure 3

(A)

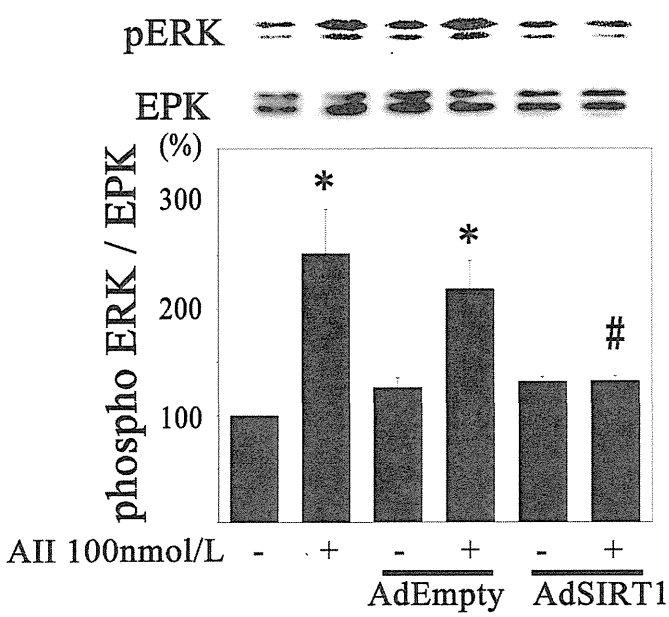

(B)

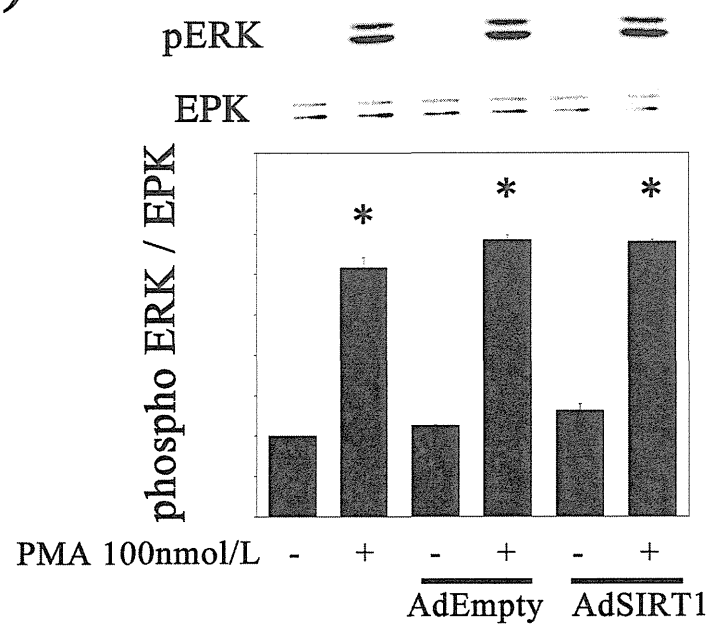

Legends for supplementary figure.

Supplementary Figure 1. Resveratrol did not affect SIRT1 expression level. : VSMCs were incubated with resveratrol (100μmol/L) for varying periods indicated in the figure (N=3). Expression of SIRT1 protein and α–tubulin was detected by Western blot analysis. The bar graph indicates the ratio of AT1R to α-tubulin. Values are expressed as a percent of control (C) culture (100%). n.s: not significant.

Supplementary Figure 2. Resveratrol suppressed AT1R mRNA expression in the presence of trichostatin A. VSMCs were pretreated with or without trichostatin A (TSA, 1μmol/L) for 24 hours and then incubated in presence or absence of resveratrol (RV, 100μmol/L) for 12 hours. Expression of AT1R mRNA was examined by Northern blot analysis. Values are expressed as a percent of control (C) culture (100%) (N=8). **P<0.01 vs control.

Supplementary Figure 3. AngII-induced ERK phosphorylation after overexpression of SIRT1. VSMCs were infected with AdSIRT1 (30moi) or AdEmpty (30moi). A, Forty eight hours after infection, the cells were incubated with or without AngII (100nM) for 5 minutes. B, The cells were incubated with or without PMA (100nM) for 5 minutes. Phosphorylation of ERK and EPK protein expression were detected by Western blot analysis. Values are expressed as a percent of control culture (100%). *P<0.01 vs Control, $^{\#}$P<0.01 vs Ad Empty+AII.

Supplementary Table 1. Body weight, heart rate and blood pressure of control and resveratrol-treated mice.

	Control (n=5)		Resveratrol (n=5)	
	before	1week	before	1week
BW(g)	25.00±0.59	25.26±0.77	25.56±0.47	25.67±0.59
HR(bpm)	468±18	467±21	481±10	461±13
SBP(mmHg)	103.1±1.6	102.6±2.3	103.1±3.0	105.4±2.1

BW, body weight; HR, heart rate; SBP, systolic blood pressure; Values are mean±SEM

Supplementary table 2. Body weight, heart rate and blood pressure of AngII and resveratrol-treated mice.

	AII+vehicle (n=5)		AII+Resveratrol (n=5)	
	before	2weeks	before	2weeks
BW(g)	23.27±0.75	25.28±1.01	23.55±0.29	25.01±0.66
HR(bpm)	479±21	496±21	500±17	507±27
SBP(mmHg)	97.9±3.2	125.9±5.5	98.4±3.3	96.9±7.7

BW, body weight; HR, heart rate; SBP, systolic blood pressure; Values are mean±SEM

Free Radical Research, April 2008; 42(4): 305–311

informa
healthcare

Effect of anaesthesia-induced alterations in haemodynamics on *in vivo* kinetics of nitroxyl probes in electron spin resonance spectroscopy

TAKAKI TSUTSUMI[1], TOMOMI IDE[1], MAYUMI YAMATO[2], MAKOTO ANDOU[1], TAKESHI SHIBA[2], HIDEO UTSUMI[3], & KENJI SUNAGAWA[1]

[1]*Department of Cardiovascular Medicine, Graduate School of Medical Sciences,* [2]*Department REDOX Medicinal Science, and* [3]*Department of Biofunctional Science, Graduate School of Pharmaceutical Sciences, Kyushu University, Fukuoka, Japan*

Accepted by Dr E. Niki

(Received 13 November 2007; in revised form 11 February 2008)

Abstract
Although the advent of *in vivo* electron spin resonance (ESR) spectroscopy has allowed analysis of the redox status of living animals, whether the haemodynamic condition affects the signal decay rate remains unknown. Three kinds of haemodynamic conditions were generated by changing the anaesthetic dosage in mice. Haemodynamics was analysed ($n = 6$ each) and *in vivo* ESR was performed to measure the signal decay rates of three nitroxyl spin probes (carbamoyl-, carboxy- and methoxycarbonyl-PROXYL) at the chest and head regions ($n = 6$ for each condition and probe). Haemodynamic analysis revealed negative inotropic and chronotropic effects on the cardiovascular system depending on the depth of anaesthesia. Although signal decay rates differed among three probes, they were not affected by heart rate alteration. In this study we report the haemodynamics-independent signal decay rate of nitoxyl probes.

Keywords: *ESR, nitroxide, reactive oxygen species*

Abbreviations: *BP, blood pressure; 3-carbamoyl-PROXYL, 3-carbamoyl-2,2,5,5-tetramethylpyrrolidine-1-oxyl; 3-carboxy-PROXYL, 3-carboxy-2,2,5,5-tetramethylpyrrolidine-l-oxyl; CmP, 3-carbamoyl-PROXYL; CxP, 3-carboxy-PROXYL; ESR, electron spin resonance; FS, fractional shortening; HR, heart rate; LV, left ventricle; LVEDD, left ventricular end-diastolic dimension; LVEDP, left ventricular end-diastolic pressure; LVESD, left ventricular end-systolic dimension; 3-methoxycarbonyl-PROXYL, 3-methoxycarbonyl-2,2,5,5-tetramethylpyrrolidine-1-oxyl; MCP, 3-methoxycarbonyl-PROXYL; ROS, reactive oxygen species.*

Introduction

Free radicals and reactive oxygen species (ROS) are important mediators in the pathogenesis of several diseases. Experimental studies have shown that free radicals and ROS cause lipid peroxidation [1], protein oxidation [2] and DNA damage [3], resulting in cellular damage. The evaluation of ROS generation and/or redox status *in vivo* is important in understanding the pathogenic mechanisms of oxidative stress.

In the last few decades, the development of *in vivo* electron spin resonance (ESR) spectroscopy has made it possible to measure exogenously administered paramagnetic species in living animals [4,5]. Furthermore, nitroxyl radicals are used as spin probes in a variety of biological experiments in which ESR spectroscopy was used to detect ROS [6–9] and redox status [10]. The *in vivo* ESR signal decay rates of spin probes are enhanced by ROS such as hydroxy radical [3] and superoxide [11,12].

Correspondence: Tomomi Ide, MD PhD, Departmentt of Cardiovascular Medicine, Graduate School of Medical Sciences, Kyushu University, Fukuoka 812-8582 Japan. Tel: +81-92-642-5359. Fax: +81-92-642-5374. Email: tomomi_i@cardiol.med.kyushu-u.ac.jp

ISSN 1071-5762 print/ISSN 1029-2470 online
DOI: 10.1080/10715760801986542

The signal decay rate also depends on kinetic factors such as the distribution of the spin probe from blood to tissues and vice versa [13], urinary excretion via the kidney [14,15], faecal excretion via the liver and bile and transport into specific tissues/organs [15]. These factors are affected by anaesthesia-related physiological responses such as the haemodynamic changes and anaesthetics are often required in experiments using living animals. Anaesthetics are known to have significant negative inotropic effects on cardiovascular parameters [16–19]. They depress the cardiac function and decrease the peripheral vascular resistance, causing bradycardia, hypotension and decreased cardiac output. However, little is known about the effect of haemodynamic change on signal decay rates of spin probes *in vivo*.

In the present study, we evaluated whether the haemodynamic change affects the signal decay rates of spin probe *in vivo*. For this purpose, mice were anaesthetized by varying doses of pentobarbital sodium and divided into three groups of low-, intermediate- and high-heart rate (HR), which was used as an index of haemodynamic parameter.

Materials and methods

Animals and experimental protocol

Male CD-1 mice weighing 30–35 g were purchased from Kyudo Ltd. (Fukuoka, Japan). The mice were housed in a temperature- and humidity-controlled room. They were fed by a commercial diet and provided water *ad libitum*. Mice were randomly assigned to three groups: high-HR group, intermediate-HR group and low-HR group, and then anaesthetized by intraperitoneal injection of pentobarbital sodium at doses of 30, 40 and 50 mg/kg body weight, respectively ($n = 6$ in each group for *in vivo* ESR) (Figure 1. After 15 min of anaesthesia, we measured rectal temperature quickly and performed ESR analysis. We also measured their rectal temperature during ESR analysis (at 3 min after the injection of spin probe). Although rectal temperature tended to be $\sim 1^{\circ}C$ lower during EPR measurement than before, there was no statistical significance among the groups (Table I). At 30 min after the injection of pentobarbital, blood samples were taken from LV for blood gas analysis. There was no difference in blood pH, pCO_2 or pO_2 among groups. All of the procedures were done within 40 min.

All procedures and animal care were approved by the Committee on Ethics of Animal Experiment, Kyushu University Graduate School of Medical and Pharmaceutical Sciences and carried out in accordance with the Guideline for Animal Experiment, Kyushu University and the Law (No.105) and Notification (No.6) of the Government. The investigations conformed with the Guide for the Care and Use of Laboratory Animals published by the US National Institutes of Health (NIH Publication No. 85-23, revised 1996).

Chemicals

3-Carbamoyl-2,2,5,5-tetramethylpyrrolidine-1-oxyl (3-carbamoyl-PROXYL) and 3-carboxy-2,2,5,5-tetramethylpyrrolidine-1-oxyl (3-carboxy-PROXYL) were purchased from Aldrich Chemical Co. (Milwaukee, WI). 3-Methoxycarbonyl-2,2,5,5-tetramethylpyrrolidine-l-oxyl (3-methoxycarbonyl-PROXYL) was synthesized as described previously [20]. Each nitroxyl probe was dissolved in physiological saline to a final concentration of 100 mmol/L. The three isotonic probe solutions were analysed by X-band ESR and adjusted to contain the same concentration of nitroxyl radicals. All other reagents used were of the highest commercially available purity.

In vivo ESR spectroscopy

For the *in vivo* ESR measurements, 3 μL/g body weight of an isotonic PROXYL solution (100 mmol/L) was administered intravenously. ESR spectra were recorded every minute at the chest or head region using a L-band ESR spectrometer (JEOL Co. Ltd., Akishima, Japan) with a loop-gap resonator (33 mm i.d. and 30 mm in length). The power of the 1.1 GHz microwave was 10 mW. The amplitude of the 100-kHz field modulation was 0.063 mT. Signal intensity was estimated from the height of the first positive peak in the spectrum. The signal decay rate was determined from the semi-logarithmic plot of signal intensity vs time after probe injection.

ECG acquisition

Needle electrodes were inserted subcutaneously into each of the four limbs. HR was calculated from electrocardiogram that was amplified and digitized online at 200 Hz by a 12-bit analogue-to-digital converter (AIO ADA 12-32/2(CB)F; Contec Co., CA). The digitized data and HR were stored on a hard disk for subsequent off-line analysis.

Echocardiography and haemodynamics measurements

Physiological evaluation with echocardiography and left heart catheterization was conducted as an independent experiment ($n = 6$, each group). At 15 min after anaesthesia, a 7.5-MHz transducer connected to a dedicated ultrasonographic system (SSD-5500, Aloka Co., Tokyo) was applied to the left hemithorax. Two-dimensional targeted M-mode imaging was obtained from the short-axis view at a level showing the greatest left ventricular (LV)

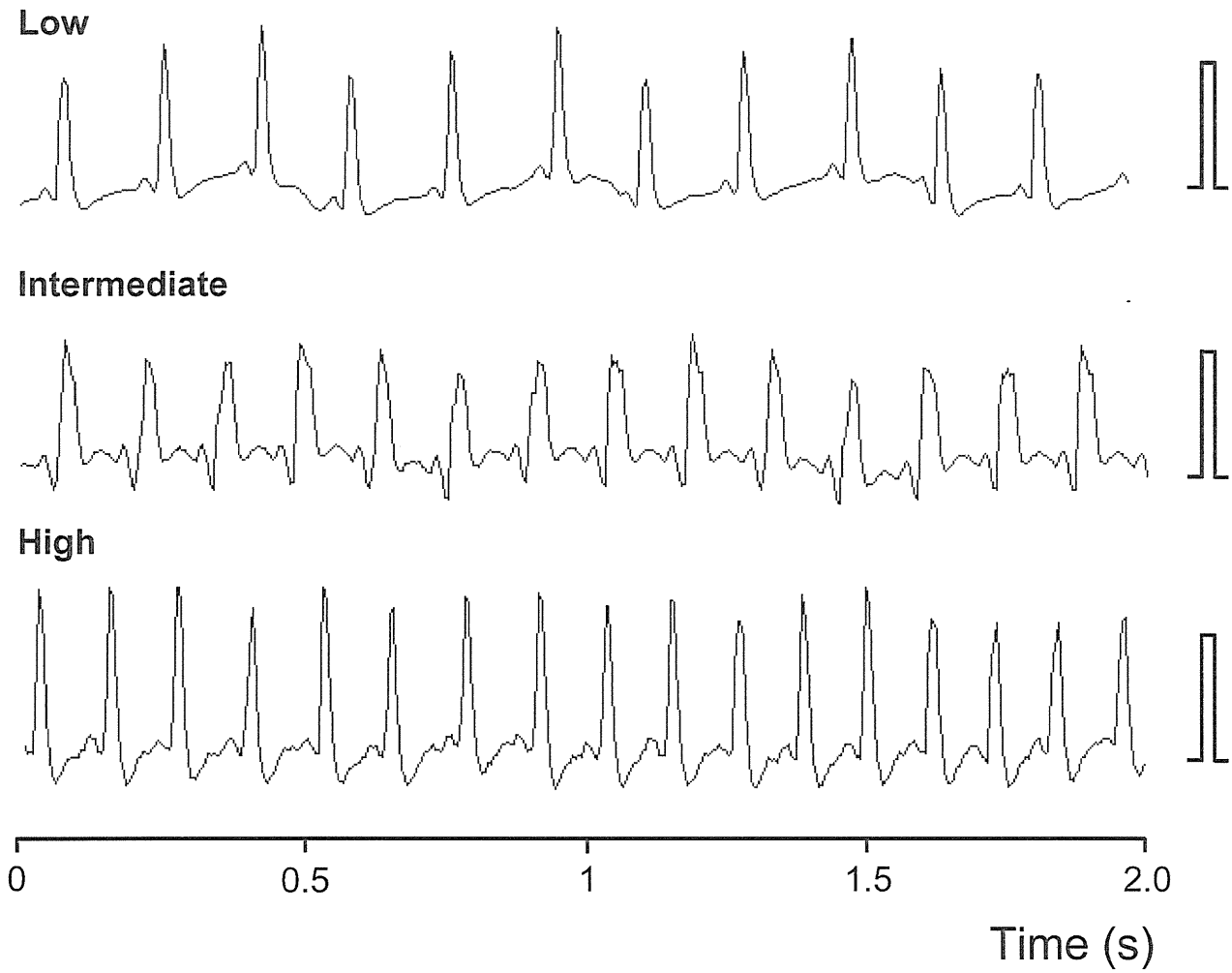

Figure 1. Typical electrocardiograms recorded from mice in the low-HR (HR: 330 bpm), intermediate-HR (HR: 420 bpm) and high-HR (HR: 510 bpm) groups. The height of the square on the right represents 1 mV.

dimension and end-diastolic (LVEDD) and end-systolic LV dimension (LVESD) were measured. Fractional shortening (FS) was calculated as follows.

$$FS\ (\%) = (LVESD - LVEDD)/LVEDD \times 100$$

After echocardiographic recording, a 1.4 F micro-manometer-tipped catheter (Millar Instruments, Houston, TX) was inserted into the right common carotid artery and advanced into the ascending aorta and LV for pressure measurement. All of the procedures ended within 40 min for each mouse.

Statistical analysis

Each value represents the mean ± SEM. Inter-group differences were analysed by one-way analysis of variance (ANOVA) followed by Tukey's post hoc test. Values of P less than 0.05 were accepted as statistically significant.

Results

HR and cardiac function

Echocardiography and left heart catheterization were performed to evaluate haemodynamics under different HR conditions induced by anaesthesia. As summarized in Table II, a marked negative inotropic and chronotropic effect on the cardiovascular system was observed dependent on the depth of anaesthesia. The HR ranged from 287–359 bpm in low-, from

Table I. Physiological variables.

	Low-HR	Intermediate-HR	High-HR
n	6	6	6
pH	7.15±0.11	7.17±0.09	7.19±0.06
P_{CO2}, mmHg	38.5±1.9	40.3±8.7	40.4±7.6
P_{O2}, mmHg	113.9±15.8	119.6±17.0	113.1±28.3
Temperature, °C (before ESR)	36.1±1.7	35.5±1.6	36.6±1.0
Temperature, °C (after ESR)	35.0±1.9	34.5±1.4	35.6±1.0

Each value represents the mean±SEM.

Table II. Characteristics of animal models.

	Low-HR	Intermediate-HR	High-HR
n	6	6	6
Heart rate, bpm	317±9	434±6*	538±8*†
Echocardiographic data			
LVEDD, mm	4.1±0.1	3.7±0.1	3.5±0.1*
LVESD, mm	2.2±0.1	1.9±0.1	1.6±0.1*
Fractional shortening, %	45±1	49±3	54±2
Haemodynamic data			
Mean BP, mmHg	65.2±4.0	83.1±4.8	101.2±2.6*†
Systolic BP, mmHg	83.1±4.1	102.0±5.4	122.0±2.3*†
Diastolic BP, mmHg	48.9±3.4	62.4±5.1	79.1±2.5*†
LVEDP, mmHg	3.5±0.4	3.1±0.7	3.2±0.7
dP/dt_{max}, mmHg/s	5890±670	8730±650	13 500±870*†
dP/dt_{min}, mmHg/s	−4510±430	−6640±310	−9 900±1190*†

LV indicates left ventricular; EDD, end-diastolic diameter; ESD, end-systolic diameter; BP, blood pressure; EDP, end-diastolic pressure. Value are mean±SEM. *$P<0.05$ vs low-HR. †$P<0.05$ vs intermediate-HR.

426–451 bpm in intermediate- and from 510–545 bpm in high-HR group. LVESD and LVEDD were significantly larger and FS was significantly lower in low-HR mice compared with high-HR mice. Aortic pressure and the first derivative of LV pressure (dP/dt_{max}) were also depressed in low-HR group compared to high-HR group. There were no significant differences in left ventricular end-diastolic pressure (LVEDP) among three groups.

In vivo *ESR spectroscopy*

ESR spectra of three spin probes (Figure 2A) were recorded at the chest or head region in mice with different haemodynamic conditions. The *in vivo* spectrum (Figure 2B) consisted of sharp triplet lines, the intensity of which decreased gradually with time after probe injection (Figure 2C). Although the rate of signal decay recorded at the chest differed among

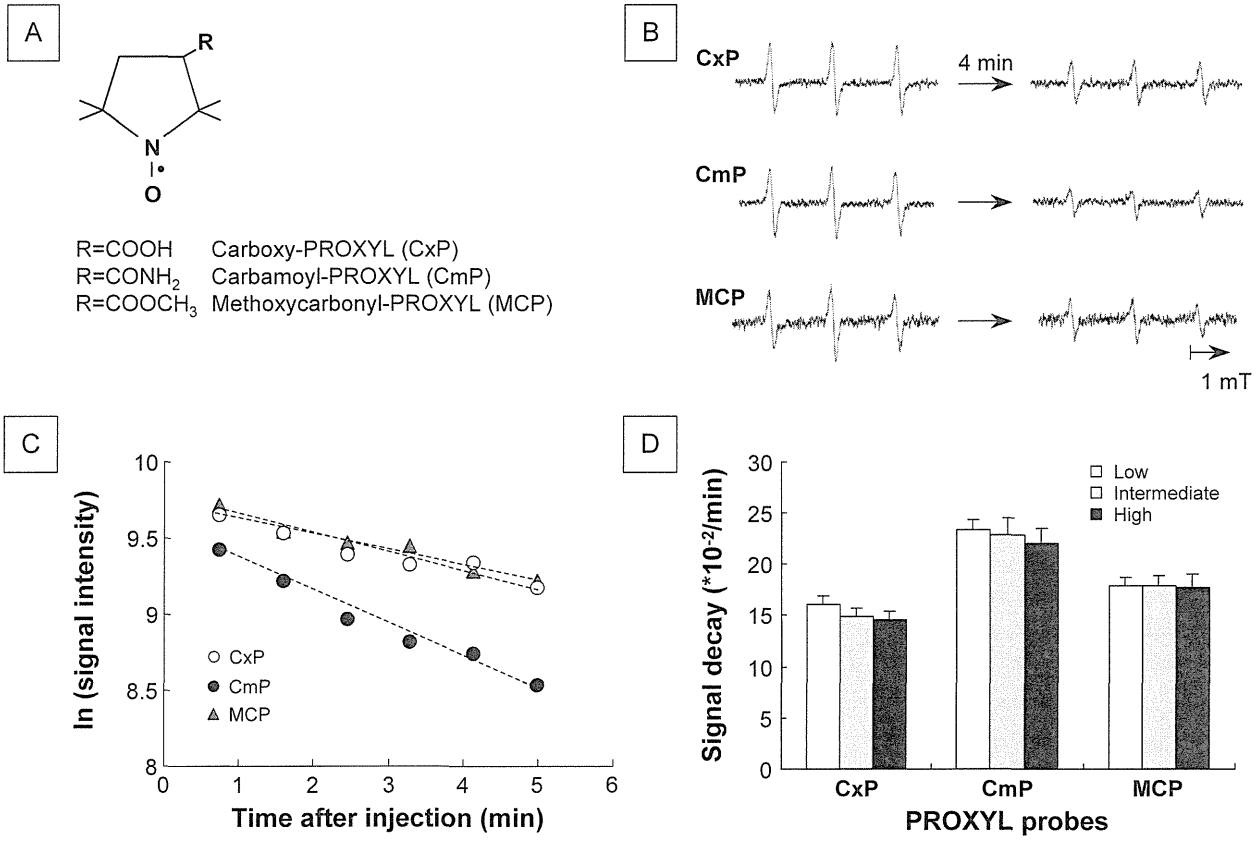

Figure 2. The chemical structure of nitroxide spin probes (A); typical ESR spectra of three spin probes (B); *in vivo* ESR signal decay curves of three spin probes from spectra recorded at chest region in the high-HR group (C); and signal decay rates of spin probes in low-HR, intermediate-HR and high-HR groups (D). Values are means±SEM. The data of (C) and (D) were obtained from six animals.

Table III. Signal deay rate at the head region ($*10^{-2}$/min).

	Low-HR	Intermediate-HR	High-HR
Carboxy-PROXYL	5.2±0.9	6.2±0.3	5.7±1.7
Carbamoyl-PROXYL	9.5±1.0	9.3±1.6	10.3±2.2
Methoxycarbonyl-PROXYL	17.5±1.3	17.0±1.3	17.6±1.5

Values are mean±SEM. No statistical significant differences among low-HR, intermediate-HR and high-HR were observed in each probe.

probes, they were not affected by the HR alteration (Figure 2D). Similarly, the signal decay is the highest with Methoxycarbonyl-PROXYL compared with the other two probes at the head level; however, HR did not affect the decay rate at all (Table III).

Discussion

Although *in vivo* ESR spectroscopy is a powerful tool to determine the free radical generation and redox status in living animals, the effect of haemodynamic change associated with the depth of anaesthesia on the decay rate of ESR signals remains unclear. In this study, we demonstrated that the signal decay rate of particular nitroxyl probes was independent of the haemodynamic condition.

The kinetics of the intravenously administered spin probes are influenced by several factors [13–15]. However, in performing *in vivo* ESR spectroscopy, spin probe has to be administered intravenously and its transport to the target organs is dependent on the blood flow. Therefore, the haemodynamic condition is considered to have considerable effect on the decay kinetics of spin probes. In this study, for the purpose of generating a broad range of haemodynamic states, we chose pentobarbital sodium among many anaesthetics, because of its wide use in experiments using rodents and its profound cardiac depressive effect compared with other intravenous or inhalation anaesthetics [19,21]. Mice were divided into three HR groups by changing the pentobarbital dosage. The average HR and dp/dt_{max} in high-HR mice were ~550 bpm and 13500 mmHg/s, respectively, which were close to the values reported in conscious mice [22]. In contrast, in mice of the low-HR group, HR and dp/dt_{max} were profoundly depressed, supporting the success of producing various haemodynamic conditions by varying the anaesthetic dose. Among these three groups, there were no significant differences in signal decay rate when each spin probe was used to acquire ESR spectra at chest and head levels.

Several mechanisms may be proposed to explain the haemodynamics-independent signal decay rate. The first factor is the acquisition of ESR spectra 30–50 s after injection of the probe. In general, the circulation time of the probes ranges from a few seconds to 1 min at the longest. Therefore, it probably takes a few seconds to a few minutes for the nitroxyl probes to reach an equilibrium state at the target organ. Takeshita et al. [23] have reported that the ESR signal obtained from mouse skin increased up to 2–3 min after injection of carbamoyl-PROXYL and then began to decrease in a first-order kinetics. However, such lag before decay was not observed in ESR spectra recorded at the chest and head levels in this study. Therefore, the time to reach equilibrium probably depends on the amount of blood supply and the vasculature structure in each organ. However, once equilibrium is achieved, the nitroxyls are reduced to reaction adduct such as secondary amine and their corresponding hydroxylamine without being affected by haemodynamics, consequently demonstrating loss of paramagnetism in a first order kinetics [24]. As we started ESR spectroscopy a few minutes after spin probe injection, the equilibrium condition has already been achieved in all groups. The second factor is the potential tissue transfer of the nitroxyl probes. Methoxycarbonyl-PROXYL is a lipophilic agent that passes through cell membrane [20,25,26]. Although carboxy-PROXYL are relatively hydrophilic [20,25,26], it was reported to be promptly taken up into tissues through the organic anion transporter [15]. Thus, a high potential of tissue transfer is also considered to be associated with the haemodynamics-independent signal decay.

There are a couple of unresolved questions in this study. First, there is a possibility that haemodynamic effects may induce biochemical alteration in longer period. Since we observed only a short-term change, further investigation is necessary for the long-time assessment. Secondly, we observe a slight tendency of the HR dependent decrease of the signal decay in carboxy-PROXYL and carbamoyl-PROXYL but not in MC-PROXYL. This might be due to the hydrophobicity of the spin probes. To clear this, we need to repeat a similar experiment in animals with more extreme conditions, which may be technically difficult in small animals.

On the other hand, there are some interesting observations in this study. After intravenous administration, the spin probes distribute from the blood to

the tissues [13], where they are reduced by enzymatic reaction [27–30]. There might be organ-specific differences in the enzymatic reduction of each probe. The order of clearance constant at the chest was as follows: carboxy- < methoxycarbonyl- < carbamoyl-PROXYL. In contrast, methoxycarbonyl-PROXYL showed the fastest signal decay rate at the head. Although the mechanisms of these differences were not elucidated in this study, the determinants of signal decay rate of each probe may depend not only on the target organs but also on the characteristics of the probe. Further studies are required to clarify these differences between spin probes.

In Conclusion, the haemodynamic condition does not affect the decay rate of ESR signal when using the *in vivo* ESR spectroscopy spin probe method. The variation in HR by anaesthetics may be compensated by homeostatic control *in vivo*, resulting in unaltered signal decay of spin probes.

Acknowledgements

This study was supported in part by grants from the Ministry of Education, Science and Culture, Health and Labor Sciences Research Grant for Comprehensive Research in Aging and Health Labor and Welfare of Japan, Japan Cardiovascular Research Foundation and Uehara Memorial Foundation. A part of this study was conducted in Kyushu University Station for Collaborative Research II.

References

[1] Kato N, Yanaka K, Hyodo K, Homma K, Nagase S, Nose T. Stable nitroxide Tempol ameliorates brain injury by inhibiting lipid peroxidation in a rat model of transient focal cerebral ischemia. Brain Res 2003;979:188–193.

[2] Hayashi T, Suda K, Imai H, Era S. Simple and sensitive high-performance liquid chromatographic method for the investigation of dynamic changes in the redox state of rat serum albumin. J Chromatogr B Analyt Technol Biomed Life Sci 2002;772:139–146.

[3] Offer T, Samuni A. Nitroxides inhibit peroxyl radical-mediated DNA scission and enzyme inactivation. Free Radic Biol Med 2002;32:872–881.

[4] Berliner LJ, Wan XM. *In vivo* pharmacokinetics by electron magnetic resonance spectroscopy. Magn Reson Med 1989;9:430–434.

[5] Ferrari M, Colacicchi S, Gualtieri G, Santini MT, Sotgiu A. Whole mouse nitroxide free radical pharmacokinetics by low frequency electron paramagnetic resonance. Biochem Biophys Res Commun 1990;166:168–173.

[6] Yamato M, Egashira T, Utsumi H. Application of *in vivo* ESR spectroscopy to measurement of cerebrovascular ROS generation in stroke. Free Radic Biol Med 2003;35:1619–1631.

[7] Yamada K, Nakamura T, Utsumi H. Enhanced intraarticular free radical reactions in adjuvant arthritis rats. Free Radic Res 2006;40:455–460.

[8] Kasazaki K, Yasukawa K, Sano H, Utsumi H. Non-invasive analysis of reactive oxygen species generated in NH4OH-induced gastric lesions of rats using a 300 MHz *in vivo* ESR technique. Free Radic Res 2003;37:757–766.

[9] Phumala N, Ide T, Utsumi H. Noninvasive evaluation of in vivo free radical reactions catalyzed by iron using *in vivo* ESR spectroscopy. Free Radic Biol Med 1999;26:1209–1217.

[10] Kuppusamy P, Li H, Ilangovan G, Cardounel AJ, Zweier JL, Yamada K, Krishna MC, Mitchell JB. Noninvasive imaging of tumor redox status and its modification by tissue glutathione levels. Cancer Res 2002;62:307–312.

[11] Krishna MC, Grahame DA, Samuni A, Mitchell JB, Russo A. Oxoammonium cation intermediate in the nitroxide-catalyzed dismutation of superoxide. Proc Natl Acad Sci USA 1992;89:5537–5541.

[12] Samuni A, Krishna CM, Mitchell JB, Collins CR, Russo A. Superoxide reaction with nitroxides. Free Radic Res Commun 1990;9:241–249.

[13] Takechi K, Tamura H, Yamaoka K, Sakurai H. Pharmacokinetic analysis of free radicals by *in vivo* BCM (Blood Circulation Monitoring)-ESR method. Free Radic Res 1997;26:483–496.

[14] Daryani A, Basu S, Becker W, Larsson A, Riserus U. Antioxidant intake, oxidative stress and inflammation among immigrant women from the Middle East living in Sweden: associations with cardiovascular risk factors. Nutr Metab Cardiovasc Dis 2007;17:748–756.

[15] Ichikawa K, Sato Y, Kondo H, Utsumi H. An ESR contrast agent is transported to rat liver through organic anion transporter. Free Radic Res 2006;40:403–408.

[16] Smith TL, Hutchins PM. Anesthetic effects on hemodynamics of spontaneously hypertensive and Wistar-Kyoto rats. Am J Physiol 1980;238:H539–H544.

[17] Shimosato S, Etsten BE. Effect of anesthetic drugs on the heart: a critical review of myocardial contractility and its relationship to hemodynamics. Clin Anesth 1969;3:17–72.

[18] Yang XP, Liu YH, Rhaleb NE, Kurihara N, Kim HE, Carretero OA. Echocardiographic assessment of cardiac function in conscious and anesthetized mice. Am J Physiol 1999;277:H1967–H1974.

[19] Janssen BJ, De Celle T, Debets JJ, Brouns AE, Callahan MF, Smith TL. Effects of anesthetics on systemic hemodynamics in mice. Am J Physiol Heart Circ Physiol 2004;287:H1618–H1624.

[20] Sano H, Matsumoto K, Utsumi H. Synthesis and imaging of blood-brain-barrier permeable nitroxyl-probes for free radical reactions in brain of living mice. Biochem Mol Biol Int 1997;42:641–647.

[21] Oguchi T, Kashimoto S, Yamaguchi T, Nakamura T, Kumazawa T. Is pentobarbital appropriate for basal anesthesia in the working rat heart model? J Pharmacol Toxicol Methods 1993;29:37–43.

[22] Kass DA, Hare JM, Georgakopoulos D. Murine cardiac function: a cautionary tail. Circ Res 1998;82:519–522.

[23] Takeshita K, Takajo T, Hirata H, Ono M, Utsumi H. *In vivo* oxygen radical generation in the skin of the protoporphyria model mouse with visible light exposure: an L-band ESR study. J Invest Dermatol 2004;122:1463–1470.

[24] Utsumi H, Muto E, Masuda S, Hamada A. *In vivo* ESR measurement of free radicals in whole mice. Biochem Biophys Res Commun 1990;172:1342–1348.

[25] Sano H, Naruse M, Matsumoto K, Oi T, Utsumi H. A new nitroxyl-probe with high retention in the brain and its application for brain imaging. Free Radic Biol Med 2000; 28:959–969.

[26] Yamato M, Egashira T, Utsumi H. Application of *in vivo* ESR spectroscopy to measurement of cerebrovascular ROS generation in stroke. Free Radic Biol Med 2003;35:1619–1631.

[27] Iannone A, Tomasi A, Vannini V, Swartz HM. Metabolism of nitroxide spin labels in subcellular fraction of rat liver. I. Reduction by microsomes. Biochim Biophys Acta 1990; 1034:285–289.

[28] Iannone A, Tomasi A, Vannini V, Swartz HM. Metabolism of nitroxide spin labels in subcellular fractions of rat liver. II. Reduction in the cytosol. Biochim Biophys Acta 1990; 1034:290–293.

[29] Quintanilha AT, Packer L. Surface localization of sites of reduction of nitroxide spin-labeled molecules in mitochondria. Proc Natl Acad Sci USA 1977;74:570–574.

[30] Utsumi H, Shimakura A, Kashiwagi M, Hamada A. Localization of the active center of nitroxide radical reduction in rat liver microsomes: its relation to cytochrome P-450 and membrane fluidity. J Biochem (Tokyo) 1989;105:239–244.

Clinical and Experimental Hypertension, 30:3–11, 2008

ISSN: 1064-1963 print / 1525-6006 online
DOI: 10.1080/10641960701813429

informa
healthcare

Atorvastatin Reduces Oxidative Stress in the Rostral Ventrolateral Medulla of Stroke-Prone Spontaneously Hypertensive Rats

TAKUYA KISHI, YOSHITAKA HIROOKA, HIROAKI SHIMOKAWA, AKIRA TAKESHITA, AND KENJI SUNAGAWA

Department of Cardiovascular Medicine, Kyushu University Graduate School of Medical Sciences, Fukuoka, Japan

Previously, we demonstrated that atorvastatin has sympatho-inhibitory effects with the upregulation of nitric oxide synthase in the brain in stroke-prone spontaneously hypertensive rats (SHRSP), and that reactive oxygen species in the rostral ventrolateral medulla (RVLM), where the vasomotor center is located, mediate the sympatho-excitatory effect. The aim of the present study was to determine if atorvastatin reduces oxidative stress in the RVLM of SHRSP along with the sympatho-inhibitory effect. SHRSP and Wistar-Kyoto (WKY) rats received standard feed with atorvastatin (50mg/kg per day) or standard feed for 30 days. Systolic blood pressure and heart rate were evaluated using the tail-cuff method. Urinary norepinephrine excretion was measured for 24 hours. After 30 days in SHRSP, blood pressure and urinary norepinephrine excretion were significantly lower in the atorvastatin group than in the control group. Thiobarbituric acid-reactive substance (TBARS) levels in the RVLM tissue obtained using the micropunch technique were used as measures of oxidative stress. Prior to the treatment, TBARS levels in the RVLM of SHRSP were significantly higher than those of WKY. After 30 days, TBARS levels in the RVLM of SHRSP were significantly lower in the atorvastatin group than in the control group. After 30 days in WKY, however, there were no differences in blood pressure, urinary norepinephrine excretion, and TBARS levels between the atorvastatin and control groups. These results suggest that atorvastatin reduces oxidative stress in the RVLM of SHRSP, which might contribute to the sympatho-inhibitory effects of atorvastatin in SHRSP.

Keywords statin, hypertension, brain, oxidative stress, sympathetic nervous system

Submitted July 16, 2005; accepted February 27, 2007.

Address correspondence to Yoshitaka Hirooka, M.D., Ph.D., Department of Cardiovascular Medicine, Kyushu University Graduate School of Medical Sciences, 3-1-1 Maidashi, Higashi-ku, Fukuoka 812-8582, Japan; E-mail: hyoshi@cardiol.med.kyushu-u.ac.jp

Introduction

Oxidative stress is implicated in the pathogenesis of hypertension (1,2). Among the target organs of hypertensive vascular diseases, the brain is the most affected by oxidative stress (3,4). Previously, we demonstrated that the generation of reactive oxygen species (ROS) is enhanced in the rostral ventrolateral medulla (RVLM) of the brain stem (i.e., where the vasomotor center is located) of stroke-prone spontaneously hypertensive rats (SHRSP), and that the oxidative stress in the RVLM induces a sympatho-excitatory effect (5). These findings suggest that oxidative stress in the RVLM is an important target in the treatment of hypertension.

The 3-hydroxy-3-methylglutaryl coenzyme A (HMG-CoA) reductase inhibitors (statins) are potent inhibitors of cholesterol biosynthesis. These agents slow the progression and foster the regression of atherosclerosis, resulting in an improvement of cardiovascular outcomes in humans with elevated and normal serum cholesterol levels (6–9). Moreover, statins might activate endothelial nitric oxide synthase (eNOS), improve endothelial function, increase vascular nitric oxide (NO) bioavailability, reduce oxidative stress, and improve endothelial progenitor cell function as a pleiotropic effect (10–19). In humans, four weeks of simvastatin treatment improves endothelial function independently of the decreases in LDL cholesterol, at least in part by reducing oxidative stress (20). The oral administration of atorvastatin has sympatho-inhibitory effects in SHRSP via an increase in NO production with upregulation of eNOS in the brain (21). The increase in NO production in the brain is thought to be mediated not only by eNOS upregulation in the brain by atorvastatin, but also by the antioxidant effect of atorvastatin, because NO is scavenged by ROS and statin has an antioxidant effect (10–19). Therefore, the aim of the present study was to determine if atorvastatin reduces oxidative stress in the RVLM of SHRSP along with the sympatho-inhibitory effect.

Materials and Methods

This study was reviewed and approved by the committee on ethics of Animal Experiments, Kyushu University Graduate School of Medical Sciences, and conducted according to the Guidelines for Animal Experiments of Kyushu University.

Measurements of Blood Pressure, Heart Rate, and Urinary Norepinephrine Excretion

Male Wister-Kyoto (WKY)/Izm and SHRSP/Izm (15 weeks old, SLC Japan, Hamamatsu, Japan) were put on standard feed or on standard feed supplemented with atorvastatin (gift from Pfizer Pharmaceuticals Inc.) and had free access to drinking water. The animals received atorvastatin at a dose of 50 mg/kg body weight per day, which was calculated according to the daily food intake (11,21), for 30 days. In rats, this dose produces plasma concentrations that are comparable to those achieved after the oral administration of similar doses of atorvastatin in humans (22). Systolic blood pressure (SBP) and heart rate (HR) were recorded using the tail-cuff method. Urine was collected for 24 hours using a metabolic cage, as described in our previous studies (5,21,23–26). Urinary norepinephrine was measured for 24 hours as a parameter of sympathetic nerve activity (5,21,23–26). To obtain RVLM tissues, the rats were deeply anesthetized with sodium pentobarbital (100 mg/kg IP) and transcardially perfused with phosphate buffered saline (5,21). The brain was removed quickly, and